

# GPrune-LLM: Generalization-Aware Structured Pruning for Large Language Models

Xiaoyun Liu<sup>1</sup>, Divya Saxena<sup>2</sup>, Jiannong Cao<sup>1</sup>, Yuqing Zhao<sup>1</sup>, Yiyang Dong<sup>1</sup>,  
and Penghui Ruan<sup>1</sup>

<sup>1</sup> Department of Computing, The Hong Kong Polytechnic University, Hong Kong  
xiaoyun.liu@connect.polyu.hk, csjcao@comp.polyu.edu.hk,  
csyzhao1@comp.polyu.edu.hk, yiyang.dong@comp.polyu.edu.hk,  
penghui.ruan@connect.polyu.hk

<sup>2</sup> School of Artificial Intelligence and Data Science, IIT Jodhpur, Jodhpur 342030,  
India  
divyasaxena@iitj.ac.in

**Abstract.** Structured pruning is widely used to compress large language models (LLMs), yet its effectiveness depends heavily on neuron importance estimation. Most existing methods estimate neuron importance from activation statistics on a single calibration dataset, which introduces calibration bias and degrades downstream cross-task generalization. We observe that neurons exhibit heterogeneous distribution sensitivity, with distribution-robust neurons maintaining consistent rankings across datasets and distribution-sensitive neurons showing high cross-dataset ranking variance. Based on this, we identify two structural limitations in existing methods. First, ranking all neurons within a shared space causes distribution-sensitive neurons that strongly activate on calibration inputs to dominate, crowding out distribution-robust neurons critical for out-of-distribution tasks. Second, applying activation-based importance metrics uniformly can be unreliable. Distribution-sensitive neurons that infrequently activate on calibration data receive insufficient activation signal for accurate local ranking. To address these limitations, we propose GPrune-LLM, a generalization-aware structured pruning framework that explicitly accounts for neuron differences in cross-distribution behavior. We first partition neurons into behavior-consistent modules to localize ranking competition, then evaluate activation-based metric reliability per module according to distribution sensitivity and score magnitude. For modules where activation-based scoring is unreliable, we switch to an activation-independent metric. Finally, we adaptively learn module-wise sparsity. Extensive experiments across multiple downstream tasks demonstrate GPrune-LLM’s consistent improvements in post-compression generalization, particularly at high sparsity, and reduced dependence on importance metric choice.

**Keywords:** Model Compression · Structured Pruning · Large Language Model

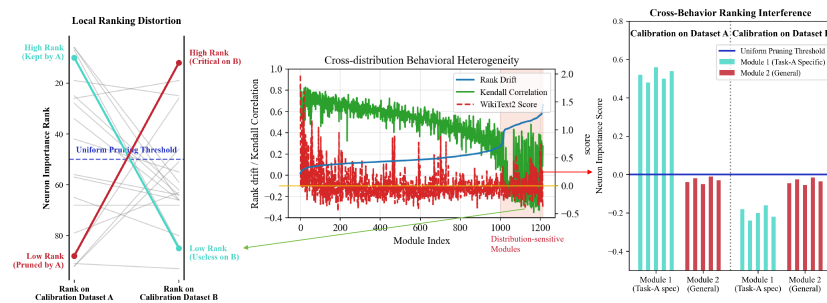


Fig. 1: Two structural limitations of activation-based structured pruning. **Middle:** Cross-distribution behavioral heterogeneity. Per-module rank drift and Kendall correlation across datasets show that many modules maintain consistent importance rankings across distributions (distribution-robust), while some exhibit high rank drift and near-zero cross-dataset correlation (distribution-sensitive). **Right:** Cross-behavior ranking interference. When task-specific and general neurons compete within a shared ranking space, task-specific neurons that strongly activate on the calibration set dominate the ranking under that calibration, suppressing distribution-robust neurons that are broadly important across tasks. **Left:** Local ranking distortion. Neurons in distribution-sensitive modules that activate infrequently on calibration data receive insufficient activation signal for reliable local ranking.

## 1 Introduction

Large language models (LLMs) have become a general backbone for a wide range of language understanding, reasoning, and generation tasks [34, 15]. Beyond pure text, multimodal models like vision-language models (VLMs) [22, 21, 35] and vision-language-action models (VLAs) [20] also widely adopt LLMs as their central reasoning backbone. As model scale continues to grow, the increasing computational and memory demands have intensified the need for effective compression. Structured pruning [26, 2, 1, 3] removes hardware-friendly units such as FFN neurons and attention heads, producing dense submodels that run efficiently on standard accelerators without requiring sparse computation kernels.

A central element in structured pruning is the effective design of importance metrics. Activation-based metrics have become the dominant choice, as they directly measure neuron utilization under realistic inputs, offering more informative signals for identifying redundant parameters than data-free alternatives [11, 33, 26, 1]. In practice, these metrics calculate activation statistics from a small calibration set. Pruning decisions are therefore implicitly conditioned on the calibration distribution, which may not represent the full range of downstream tasks. When calibration patterns diverge from the target distribution, this introduces calibration bias and degrades the generalization performance of the pruned model.

Prior studies [4,18] have empirically quantified this calibration bias, finding that calibration data selection can dominate method-level differences at high sparsity. The prevailing remedy has been data-centric by constructing more representative calibration sets through careful selection [18] or iterative augmentation [38]. Rather than further optimizing calibration data, we explore a complementary direction: Can the pruning mechanism itself be made intrinsically more resistant to calibration bias?

To answer this question, we examine how calibration bias propagates through existing activation-based pruning frameworks. We observe that neurons exhibit different cross-distribution behaviors. Some neurons maintain relatively consistent activation-based ranking across diverse datasets (distribution-robust), while others show high cross-dataset ranking variance (distribution-sensitive). This heterogeneity aligns with prior findings on the emergent modularity of FFN neurons [14,45,46,30] in which neurons naturally form co-activation groups, with modules exhibiting broader response patterns tending to be distribution-robust and those with narrower patterns tending to be distribution-sensitive. Considering this heterogeneity, we identify two structural limitations in existing methods, as shown in Fig. 1.

First, most existing methods rank all neurons within a shared space, implicitly assuming uniform comparability across neurons. Given that neurons differ in distribution sensitivity, distribution-sensitive neurons that strongly activate on calibration inputs can dominate the ranking and suppress distribution-robust neurons that are broadly important across tasks, leading to systematic over-pruning of neurons critical for out-of-distribution generalization, which we term cross-behavior ranking interference.

Second, existing methods apply activation-based metrics uniformly to all neurons, implicitly assuming activation signals are equally reliable. However, among distribution-sensitive neurons, those that activate infrequently on the calibration set receive insufficient activation signal for accurate fine-grained ranking, which we term local ranking distortion.

Motivated by these findings, we propose GPrune-LLM, a generalization-aware structured pruning framework that explicitly accounts for neuron differences in cross-distribution behavior to reduce calibration bias. To mitigate cross-behavior ranking interference, we first partition FFN neurons into behavior-consistent modules by jointly modeling neuron parameter similarity and cross-dataset rank drift. This confines ranking competition to neurons with compatible distribution sensitivity. Building on these modules, we evaluate the reliability of activation-based importance metrics per module using each module’s distribution sensitivity and score magnitude. We then adapt importance metrics based on metric reliability to resolve local ranking distortion, with module-wise sparsity learned adaptively under a global budget.

Our contributions are as follows:

1. We conduct a mechanism-centric analysis of how calibration bias propagates through existing activation-based methods in LLM structured pruning, finding that neurons exhibit heterogeneous distribution sensitivity, and identify-

- ing two structural limitations in existing methods that arise from neglecting it, namely cross-behavior ranking interference and local ranking distortion.
2. We propose GPrune-LLM, a generalization-aware structured pruning framework that explicitly considers neuron cross-distribution behavioral differences and directly targets both identified limitations via behavior-consistent modularization and reliability-aware modular pruning. GPrune-LLM is plug-and-play with existing importance metrics.
  3. Extensive experiments on various models across multiple compression ratios demonstrate that GPrune-LLM consistently improves post-compression generalization over state-of-the-art baselines, with particularly pronounced gains at high sparsity, and substantially reduces dependence on the choice of importance metric.

## 2 Related Works

### 2.1 LLM Pruning

LLM pruning falls into two categories: unstructured and structured variants. Unstructured methods zero out individual weights, differing in both importance metrics [11,33,9] and sparsity allocation strategies [39,6]. However, practical speedup depends on hardware support for sparse execution.

Structured pruning removes entire architectural units for dense-hardware acceleration. Existing methods primarily focus on improving structure identification, importance estimation, sparsity allocation and accuracy recovery. LLM-Pruner [26] discovers structurally coupled groups via gradient approximations and recovers accuracy with LoRA fine-tuning. SliceGPT [2] takes a complementary approach, applying orthogonal transformations to reduce hidden dimensions directly. LoRAPrune [44] unifies pruning guidance with parameter-efficient adaptation via LoRA gradient signals. Coupled structure selection [43] extends dependency modeling to improve structure identification, while reconstruction-based calibration [36] minimizes post-pruning output deviation to recover accuracy. FLAP [1] introduces a fluctuation-based metric to estimate neuron importance, and standardizes scores across layers for global sparsity allocation, with bias compensation to restore pruned layer output. GAP [3] formalizes global sparsity allocation as an optimization problem, jointly determining per-layer pruning ratios under a budget constraint via dynamic programming.

Our work addresses an orthogonal problem of calibration bias by considering cross-distribution behavioral differences among neurons and restructuring the ranking space for generalization-aware pruning.

### 2.2 Calibration Bias in LLM Pruning

Activation-based importance metrics [33,11,1] are widely used in LLM pruning, as activations directly reflect neuron usage. However, these metrics condition rankings on a small calibration set, making importance rankings biased by calibration distribution.

This calibration bias has recently attracted dedicated study. Williams and Aletras [37] systematically analyze how calibration data composition affects both quantization and pruning outcomes, finding substantial task-dependent variability. Bandari *et al.* [4] investigate the optimality of C4 as a default calibration dataset and find that calibration choice can dominate method differences at high sparsity. Ji *et al.* [18] further show that changing calibration data can substantially alter pruning outcomes.

These findings have motivated a data-centric line of work that improves the calibration set. Ji *et al.* [18] develop task-aligned calibration selection strategies to better match the calibration distribution to target tasks. Wu *et al.* [38] propose iterative pruning with multi-domain calibration to broaden distributional coverage.

Our work takes a mechanism-centric direction, focusing on improving the pruning mechanism itself to reduce calibration-induced bias. A concurrent work, FANG [40], also explores LLM generalization in structured pruning from a mechanism perspective. Motivated by functional specialization [14,45,46,30], it groups neurons by functional roles inferred from semantic context clustering on a single calibration dataset and reweights token contributions within each group. Our work targets a different dimension. We partition neurons by cross-distribution behavioral pattern to restructure the ranking space and assess per-module metric reliability. Since single-dataset activation patterns may be biased by that dataset’s language distribution, we jointly model data-free parameter similarity as a proxy for co-activation affinity and cross-dataset rank drift for distribution sensitivity, yielding more general behavioral modules.

### 3 Methodology

In this section, we introduce GPrune-LLM, which consists of two main stages: Behavior-consistent Modularization and Reliability-Aware Modular Pruning. The overview is illustrated in Fig. 2 and summarized in Algorithm 1.

#### 3.1 Behavior-consistent Modularization

The goal of Behavior-consistent Modularization is to partition FFN neurons into modules whose neurons exhibit consistent sensitivity to diverse input distributions. Co-activation affinity is a natural grouping signal, but co-activation estimated from a single calibration set may capture dataset-specific patterns rather than intrinsic neuron behavior. We therefore jointly model two complementary signals: parameter similarity, which captures co-activation affinity independent of any specific input distribution, and cross-dataset rank drift, which directly measures the stability of each neuron’s importance ranking across distributions.

Parameter similarity [45] is a data-free co-activation proxy, as neurons with similar weight vectors produce correlated activations regardless of the input distribution. For neurons  $i$  and  $j$  with weight vectors  $\mathbf{w}_i$  and  $\mathbf{w}_j$ , the pairwise parameter similarity is:

$$a_{ij} = \cos(\mathbf{w}_i, \mathbf{w}_j). \tag{1}$$

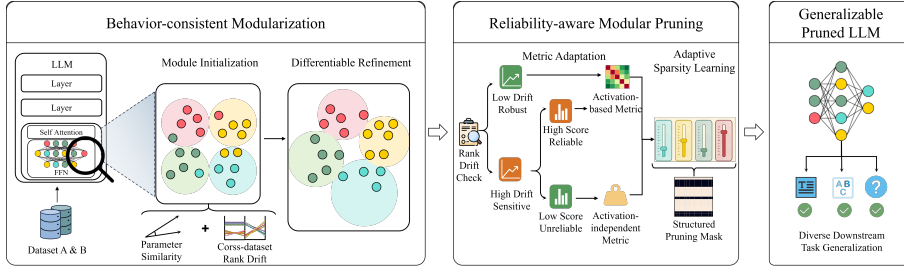


Fig. 2: Overview of GPrune-LLM. FFN neurons are first partitioned into behavior-consistent modules by jointly modeling data-free parameter similarity and cross-dataset rank drift, with assignments refined via a differentiable objective. Each module’s mean rank drift then serves as a sensitivity indicator of this module. Distribution-robust (low-drift) modules retain activation-based metrics, while distribution-sensitive (high-drift) modules with low activation scores switch to activation-independent alternatives, ensuring reliable within-module ranking. Finally, module-specific sparsity is adaptively learned, yielding a pruned LLM with improved generalization across diverse downstream tasks.

Cross-dataset rank drift captures the importance ranking shift of each neuron between datasets. For two calibration datasets  $A$  and  $B$ , the rank drift of neuron  $i$  within its layer is:

$$d_i = \frac{|r_A(i) - r_B(i)|}{N - 1}, \quad (2)$$

where  $r_A(i)$ ,  $r_B(i)$  are the within-layer activation-based ranks on each dataset and  $N$  is the layer width. Large  $d_i$  marks a distribution-sensitive neuron, small  $d_i$  a distribution-robust one. Two neurons are behavior-consistent when they are close in parameter space and share similar rank drift profiles.

**Module Initialization** We initialize modules in two steps to incorporate both parameter similarity and rank drift information.

First, we cluster neurons by cosine similarity using KMeans [24], and select the number of modules  $K$  with a silhouette criterion. This groups neurons with implicit co-activation affinity while remaining free from calibration bias.

Second, we split modules with high rank drift heterogeneity. For each module  $\mathcal{C}_k$ , we compute the within-module drift standard deviation  $\sigma_k = \text{std}(\{d_i\}_{i \in \mathcal{C}_k})$ . A global split threshold is set as  $\delta_{\text{split}} = Q_{\gamma_{\text{split}}}(\{\sigma_k\}_{k=1}^K)$ , where  $Q_{\gamma_{\text{split}}}(\cdot)$  denotes the  $\gamma_{\text{split}}$ -quantile over module-level drift standard deviations. Any module with  $\sigma_k > \delta_{\text{split}}$  is split into a low-drift (distribution-robust) subgroup and a high-drift (distribution-sensitive) subgroup, subject to a minimum subgroup size. This initialization largely separates behavioral types before differentiable refinement.

**Differentiable Refinement** Discrete initialization, however, cannot jointly optimize parameter similarity and rank drift consistency in an end-to-end manner.

We therefore refine module assignments using soft membership probabilities. For neuron  $i$ , the probability of belonging to module  $k$  is defined as:

$$p_{ik} = \text{softmax}_k(\cos(\mathbf{x}_i, \mathbf{c}_k)), \quad (3)$$

where  $\mathbf{x}_i$  is the normalized neuron parameter and  $\mathbf{c}_k$  is the module centroid. The refinement objective  $\mathcal{L}_{\text{BCDM}}$  is a weighted sum of three terms: a parameter similarity term  $\mathcal{L}_{\text{sim}}$  which combines compactness  $\mathcal{L}_{\text{inner}}$  with worst-cluster penalty  $\mathcal{L}_{\text{pair}}$ , a rank-drift consistency term  $\mathcal{L}_{\text{consis}}$ , and a repulsion term  $\mathcal{L}_{\text{rep}}$ .

$\mathcal{L}_{\text{inner}}$  promotes compact module assignments by minimizing the soft-weighted distance from each neuron to module centroids:

$$\mathcal{L}_{\text{inner}} = \frac{1}{N} \sum_{i=1}^N \sum_{k=1}^K p_{ik} (1 - \cos(\mathbf{x}_i, \mathbf{c}_k)). \quad (4)$$

To prevent a few highly dispersed modules from dominating the clustering error, we use a worst-module compactness penalty:

$$\mathcal{L}_{\text{pair}} = \frac{1}{m} \sum_{k \in \mathcal{T}_m} h_k, \quad h_k = \frac{1}{|\mathcal{C}_k|^2} \sum_{i,j \in \mathcal{C}_k} (1 - \cos(\mathbf{x}_i, \mathbf{x}_j)), \quad m = \lceil \gamma_{\text{pair}} K \rceil. \quad (5)$$

where  $h_k$  is the mean intra-module cosine distance,  $\gamma_{\text{pair}} \in (0, 1)$  controls the fraction of modules to penalize, and  $\mathcal{T}_m$  is the index set of the  $m$  modules with the largest  $h_k$ .

The rank-drift consistency term  $\mathcal{L}_{\text{consis}}$  groups neurons with similar drift profiles by minimizing the within-module variance of rank drift  $d$ :

$$\mathcal{L}_{\text{consis}} = \frac{1}{K} \sum_{k=1}^K \frac{\sum_i p_{ik} (d_i - \tilde{d}_k)^2}{\sum_i p_{ik}}, \quad \tilde{d}_k = \frac{\sum_i p_{ik} d_i}{\sum_i p_{ik}}. \quad (6)$$

where  $\tilde{d}_k$  is the soft assignment-weighted mean drift of module  $k$ . Minimizing  $\mathcal{L}_{\text{consis}}$  separates low-drift from high-drift neurons across modules, providing behavior-consistent partition for the following pruning stage.

The repulsion term  $\mathcal{L}_{\text{rep}}$  prevents module collapse by maintaining angular separation among centroids:

$$\mathcal{L}_{\text{rep}} = \frac{1}{K(K-1)} \sum_{k \neq k'} \cos^2(\mathbf{c}_k, \mathbf{c}_{k'}). \quad (7)$$

Collectively,  $\mathcal{L}_{\text{BCDM}}$  yields modules that are compact in parameter space, internally consistent in distribution sensitivity, and well-separated, providing the structural foundation for reliable modular pruning.

### 3.2 Reliability-Aware Modular Pruning

**Metric Adaptation** After modularization, each module contains neurons with similar cross-distribution behavior. We evaluate the reliability of activation-based metrics per module using two complementary indicators: mean rank drift

$\bar{d}_k$ , which captures module sensitivity across distributions, and mean activation-based score  $\bar{s}_k^{\text{act}}$ , which reflects the strength of calibration signal received by the module.

A low mean rank drift indicates a distribution-robust module with stable rankings, for which activation-based metrics are generally reliable. A high mean rank drift indicates a distribution-sensitive module where neuron rankings fluctuate across datasets, making it more susceptible to calibration bias. However, a sensitive module with high mean activation score has received sufficient calibration signal, making activation-based ranking still reliable within the module. Metric replacement is therefore needed only when high rank drift is accompanied by low mean activation score.

We adapt metrics using two quantile-based thresholds:

$$\delta_{\text{drift}} = Q_{\gamma_{\text{drift}}}(\{\bar{d}_k\}_{k=1}^K), \quad \delta_{\text{score}} = Q_{\gamma_{\text{score}}}(\{\bar{s}_k^{\text{act}}\}_{k=1}^K), \quad (8)$$

where  $\gamma_{\text{drift}}, \gamma_{\text{score}} \in (0, 1)$  are percentile ratios.

$$s_i = \begin{cases} s_i^{\text{ind}}, & \bar{d}_{k(i)} > \delta_{\text{drift}} \text{ and } \bar{s}_{k(i)}^{\text{act}} < \delta_{\text{score}}, \\ s_i^{\text{act}}, & \text{otherwise,} \end{cases} \quad (9)$$

where  $s_i^{\text{act}}$  is the score of an activation-based metric (e.g., FLAP) and  $s_i^{\text{ind}}$  is that of an activation-independent metric (e.g., weight-norm).

**Adaptive Sparsity Learning** Inspired by dynamic sparse training [19], we learn module-specific thresholds  $\tau_k$  so that each module adapts its sparsity to its local score landscape. For attention heads, which are not modularized, a single threshold  $\tau_\ell^{\text{attn}}$  is learned per layer. For neuron  $i$  in module  $k(i)$ , the pruning mask is computed as:

$$m_i = S(s_i - \tau_{k(i)}), \quad S(x) = \begin{cases} 1 & x \geq 0 \\ 0 & x < 0 \end{cases} \quad (10)$$

where  $S(\cdot)$  is the non-differentiable binary step function. We apply a straight-through estimator (STE) [17], using a smooth surrogate in the backward pass to propagate gradients to the thresholds.

The optimization objective  $\mathcal{L}_{\text{prune}}$  consists of two components: a performance term  $\mathcal{L}_{\text{perf}}$  and a sparsity-constraint term  $\mathcal{L}_{\text{constr}}$ .  $\mathcal{L}_{\text{perf}}$  combines cross-entropy and knowledge distillation [16] from the unpruned model to preserve task capability.  $\mathcal{L}_{\text{constr}}$  anchors the global retention ratio to the target  $r^*$  throughout threshold learning.

A fixed penalty with uniform correction can cause oscillation near the target and slow convergence when far from it. We therefore adopt an augmented Lagrangian formulation. Let  $g = \hat{r} - r^*$  denote the deviation from the target retention ratio, where  $\hat{r}$  is the estimated retention ratio from the STE masks. The sparsity-constraint term is:

$$\mathcal{L}_{\text{constr}} = \lambda_c g + \frac{\rho}{2} g^2, \quad (11)$$

---

**Algorithm 1** GPrune-LLM Pipeline

---

**Require:** Pretrained model  $M$ , calibration datasets  $A, B$ , target retention ratio  $r^*$ , candidate module numbers  $\mathcal{K}$ , penalty coefficient  $\rho$

**Ensure:** Pruned model  $M_{\text{pruned}}$

- 1: **for** each FFN layer  $\ell$  **do**
- 2:   Compute parameter similarity  $a_{ij}$  by Eq. (1)
- 3:   Compute rank drift  $d_i$  by Eq. (2) using  $A, B$
- 4:   Initialize modules by cosine KMeans based on  $\{a_{ij}\}$  and select  $K^* \in \mathcal{K}$  via silhouette criterion
- 5:   Apply rank-drift split based on  $\{d_i\}$  to separate distribution-robust and distribution-sensitive neurons
- 6:   Refine soft assignments  $p_{\ell ik}$  by minimizing  $\mathcal{L}_{\text{BCDM}}$
- 7: **end for**
- 8: **for** each FFN layer  $\ell$  **do**
- 9:   **for** each module  $\mathcal{C}_{\ell, k}$  **do**
- 10:     Compute module statistics  $\bar{d}_{\ell, k}$  and  $\bar{s}_{\ell, k}^{\text{act}}$
- 11:     Assign metric by Eq. (9) using  $(\bar{d}_{\ell, k}, \bar{s}_{\ell, k}^{\text{act}})$  to obtain neuron scores  $s_{\ell, i}$
- 12:   **end for**
- 13: **end for**
- 14: Compute attention head scores  $s_{\ell, h}^{\text{attn}}$  using the base metric
- 15: Initialize learnable thresholds  $\{\tau_{\ell, k}\}$ ,  $\{\tau_{\ell}^{\text{attn}}\}$ , dual variable  $\lambda_c \leftarrow 0$ , and target retention ratio  $r^*$
- 16: **while** not converged **do**
- 17:   Forward pass with neuron masks  $m_{\ell, i} = S(s_{\ell, i} - \tau_{\ell, k(i)})$  and attention-head masks  $m_{\ell, h}^{\text{attn}} = S(s_{\ell, h}^{\text{attn}} - \tau_{\ell}^{\text{attn}})$ , and compute  $\mathcal{L}_{\text{prune}}$
- 18:   Update  $\{\tau_{\ell, k}\}$  and  $\{\tau_{\ell}^{\text{attn}}\}$  by backpropagating  $\mathcal{L}_{\text{prune}}$  via STE surrogate
- 19:   Compute  $g = \hat{r} - r^*$  from all STE masks, and update  $\lambda_c \leftarrow \lambda_c + \rho g$
- 20: **end while**
- 21: Export hard-pruned FFN structure as  $M_{\text{pruned}}$

---

where  $\lambda_c$  is a dual variable updated as  $\lambda_c \leftarrow \lambda_c + \rho g$  after each iteration, and  $\rho$  is the quadratic penalty coefficient.

## 4 Experiments

### 4.1 Experimental Settings

We evaluate GPrune-LLM on LLaMA2-7B, LLaMA2-13B, Vicuna1.5-7B, and LLaVA1.5-7B. We compare against three structured pruning baselines: LLM-Pruner [26] (without LoRA fine-tuning), Wanda [33] (structured variant, Wanda-sp[1]), and FLAP [1]. GPrune-LLM is applied on top of Wanda-sp and FLAP as base importance metrics. We denote them as GPrune-LLM (Wanda-sp) and GPrune-LLM (FLAP). No post-pruning fine-tuning is applied to any method. LLM-Pruner is excluded from LLaMA2-13B and LLaVA1.5-7B experiments due to GPU memory constraints.

For language models, we evaluate language modeling perplexity on Wiki-Text2 [28] and PTB [27], and zero-shot accuracy across seven commonsense

Table 1: Comparison on LLaMA2-7B. For each retention ratio, the best and second-best results are marked in **bold** and underline, respectively.  $\uparrow$  denotes improvement over the corresponding base method at the same retention ratio. For language modeling perplexity, lower is better. For classification tasks accuracy, higher is better.

Ratio Method	WikiText2	PPL	PTB	PPL	BoolQ	PIQA	HellaSwag	WinoGrande	ARC-e	ARC-c	OBQA	Avg	Acc
100% LLaMA2-7B	12.19	48.35	71.10	78.40	72.96	67.25	69.36	40.53	40.80	62.91			
80% LLM-Pruner	19.23	72.62	62.26	<u>76.28</u>	65.82	60.85	63.85	<u>37.46</u>	<u>39.20</u>	<u>57.96</u>			
Wanda-sp	17.50	67.01	46.79	<b>76.50</b>	<u>68.13</u>	<b>65.43</b>	<b>65.95</b>	<b>39.76</b>	38.20	57.25			
GPrune-LLM (Wanda-sp)	<u>15.92</u> $\uparrow$	<u>60.29</u> $\uparrow$	<u>62.69</u> $\uparrow$	75.52	<b>68.42</b> $\uparrow$	<u>65.27</u>	<u>63.97</u>	<u>37.46</u>	<b>39.60</b> $\uparrow$	<b>58.99</b> $\uparrow$			
FLAP	16.41	61.61	52.45	73.61	62.56	62.12	59.13	34.81	<u>39.20</u>	54.84			
GPrune-LLM (FLAP)	<b>15.27</b> $\uparrow$	<b>59.93</b> $\uparrow$	<b>65.66</b> $\uparrow$	74.65 $\uparrow$	66.55 $\uparrow$	59.98	63.76 $\uparrow$	35.24 $\uparrow$	<u>39.20</u>	57.86 $\uparrow$			
70% LLM-Pruner	29.40	111.56	50.15	71.82	55.64	55.49	54.67	31.57	36.40	50.82			
Wanda-sp	22.94	79.79	<u>58.78</u>	71.49	59.44	55.56	<u>60.27</u>	<u>37.03</u>	<b>39.40</b>	54.57			
GPrune-LLM (Wanda-sp)	20.46 $\uparrow$	76.31 $\uparrow$	57.74	<b>72.52</b> $\uparrow$	<b>63.08</b> $\uparrow$	<u>59.51</u> $\uparrow$	<b>60.82</b> $\uparrow$	<b>37.20</b> $\uparrow$	38.80	<b>55.67</b> $\uparrow$			
FLAP	<u>20.25</u>	<u>76.02</u>	53.39	69.48	55.49	<b>60.30</b>	54.71	32.59	38.20	52.02			
GPrune-LLM (FLAP)	<b>18.02</b> $\uparrow$	<b>69.96</b> $\uparrow$	<b>63.24</b> $\uparrow$	<u>72.36</u> $\uparrow$	<u>60.71</u> $\uparrow$	56.91	58.12 $\uparrow$	33.96 $\uparrow$	<u>39.00</u> $\uparrow$	<u>54.90</u> $\uparrow$			
50% LLM-Pruner	227.85	459.50	<b>60.61</b>	58.43	30.56	49.33	31.19	27.05	31.40	41.22			
Wanda-sp	262.32	505.51	<u>59.82</u>	54.13	26.54	49.41	29.00	23.89	32.80	39.37			
GPrune-LLM (Wanda-sp)	50.65 $\uparrow$	172.26 $\uparrow$	56.70	<u>63.11</u> $\uparrow$	<u>43.84</u> $\uparrow$	<u>51.46</u> $\uparrow$	<u>40.74</u> $\uparrow$	<b>30.63</b> $\uparrow$	<b>35.60</b> $\uparrow$	<b>46.01</b> $\uparrow$			
FLAP	<u>42.81</u>	<u>152.49</u>	39.63	62.13	39.54	50.36	35.52	28.24	<u>35.20</u>	41.52			
GPrune-LLM (FLAP)	<b>33.92</b> $\uparrow$	<b>129.06</b> $\uparrow$	51.13 $\uparrow$	<b>63.60</b> $\uparrow$	<b>45.01</b> $\uparrow$	<b>52.49</b> $\uparrow$	<b>43.52</b> $\uparrow$	<u>29.35</u> $\uparrow$	34.80	<u>45.70</u> $\uparrow$			

benchmarks, i.e., BoolQ [7], PIQA [5], HellaSwag [42], WinoGrande [32], ARC-Easy, ARC-Challenge [8], and OBQA [29], using the EleutherAI LM Evaluation Harness [13]. For LLaVA1.5-7B, we report multimodal benchmark scores on IE-Perception and IE-Reasoning from MME [12], MMBench [23], MMMU [41], and ScienceQA [25], using VLMEvalKit [10], and summarize overall retention as Rel (%). Retention ratios range from 80% to 50% for 7B models, 50%–30% for LLaMA2-13B, and 90%–80% for LLaVA1.5-7B. For LLaMA2-13B, most methods perform comparably at mild sparsity, so we focus on the more challenging 50%–30% range where performance differences are more informative. For LLaVA1.5-7B, the multimodal architecture is more sensitive to structured pruning, and aggressive sparsity causes complete collapse of base metrics, so we evaluate at 90%–80% where meaningful comparison is possible.

Following prior work [1], we set the sequence length to 128, and use WikiText2 as the primary calibration dataset with 2048 samples for importance scoring and sparsity learning. PTB serves as the auxiliary dataset solely for computing rank drift to infer neuron behavior during modularization and does not directly contribute to importance scores or sparsity decisions, which ensures relatively fair comparison with single-dataset baselines. All experiments are conducted on a single NVIDIA RTX A6000 48GB GPU. On LLaMA2-7B, behavior-consistent modularization completes in approximately one hour, and each threshold training epoch in adaptive sparsity learning takes around 0.5 hour.

Additional results on LLaMA1-7B, more extreme sparsity ratios for LLaMA2-7B, and detailed experimental settings are provided in the supplementary material.

Table 2: Comparison on Vicuna1.5-7B.

Ratio Method	WikiText2	PPL	PTB	PPL	BoolQ	PIQA	HellaSwag	WinoGrande	ARC-e	ARC-c	OBQA	Avg Acc
100% Vicuna1.5-7B	16.24	60.78	75.75	77.80	71.02	67.64	69.02	40.87	42.40	63.50		
80% LLM-Pruner	24.90	86.20	50.98	<b>75.84</b>	64.14	59.83	66.12	<b>38.65</b>	40.00	56.51		
Wanda-sp	23.66	73.67	67.31	74.16	65.21	61.80	<b>66.96</b>	38.31	39.80	59.08		
GPrune-LLM (Wanda-sp)	21.32 $\uparrow$	<u>72.51<math>\uparrow</math></u>	<b>69.51<math>\uparrow</math></b>	<u>75.68<math>\uparrow</math></u>	<b>67.51<math>\uparrow</math></b>	<u>64.09<math>\uparrow</math></u>	<u>66.37</u>	<u>38.48<math>\uparrow</math></u>	<u>40.20<math>\uparrow</math></u>	<b>60.26<math>\uparrow</math></b>		
FLAP	<u>21.06</u>	76.42	66.88	72.47	63.17	<b>64.48</b>	63.55	34.81	39.80	57.88		
GPrune-LLM (FLAP)	<b>19.27<math>\uparrow</math></b>	<b>72.15<math>\uparrow</math></b>	<u>67.80<math>\uparrow</math></u>	<u>75.63<math>\uparrow</math></u>	<u>66.70<math>\uparrow</math></u>	63.46	<b>66.96<math>\uparrow</math></b>	38.05 $\uparrow$	<b>41.00<math>\uparrow</math></b>	<u>59.94<math>\uparrow</math></u>		
70% LLM-Pruner	36.44	120.82	43.94	<u>73.45</u>	56.13	57.30	58.89	34.30	38.20	51.74		
Wanda-sp	32.49	98.83	44.01	71.33	57.85	56.51	<u>62.21</u>	<u>37.12</u>	38.80	52.55		
GPrune-LLM (Wanda-sp)	27.40 $\uparrow$	98.01 $\uparrow$	<b>66.97<math>\uparrow</math></b>	73.29 $\uparrow$	<u>62.12<math>\uparrow</math></u>	<u>61.97<math>\uparrow</math></u>	61.49	36.86	<u>39.00<math>\uparrow</math></u>	<u>57.39<math>\uparrow</math></u>		
FLAP	<u>25.26</u>	<u>90.87</u>	<u>66.18</u>	69.86	57.56	<b>62.35</b>	59.97	33.11	38.40	55.35		
GPrune-LLM (FLAP)	<b>23.28<math>\uparrow</math></b>	<b>82.30<math>\uparrow</math></b>	64.34	<b>73.67<math>\uparrow</math></b>	<b>62.55<math>\uparrow</math></b>	60.46	<b>64.81<math>\uparrow</math></b>	<b>37.63<math>\uparrow</math></b>	<b>40.40<math>\uparrow</math></b>	<b>57.69<math>\uparrow</math></b>		
50% LLM-Pruner	168.91	450.48	<b>62.39</b>	60.23	34.12	53.35	35.82	27.82	34.00	43.96		
Wanda-sp	270.82	551.68	<u>60.83</u>	56.64	27.38	50.12	29.12	23.04	31.20	39.76		
GPrune-LLM (Wanda-sp)	59.93 $\uparrow$	189.62 $\uparrow$	53.79	<u>63.98<math>\uparrow</math></u>	<u>43.67<math>\uparrow</math></u>	<b>54.85<math>\uparrow</math></b>	45.45 $\uparrow$	<b>29.44<math>\uparrow</math></b>	<b>36.00<math>\uparrow</math></b>	<u>46.00<math>\uparrow</math></u>		
FLAP	<u>50.23</u>	<u>179.31</u>	38.50	63.22	41.22	53.28	<u>46.97</u>	<u>29.35</u>	34.60	43.88		
GPrune-LLM (FLAP)	<b>41.36<math>\uparrow</math></b>	<b>148.48<math>\uparrow</math></b>	52.08 $\uparrow$	<b>65.34<math>\uparrow</math></b>	<b>44.05<math>\uparrow</math></b>	<u>53.59<math>\uparrow</math></u>	<b>52.69<math>\uparrow</math></b>	29.01	<u>35.20<math>\uparrow</math></u>	<b>47.42<math>\uparrow</math></b>		

Table 3: Comparison on LLaMA2-13B.

Ratio Method	WikiText2	PPL	PTB	PPL	BoolQ	PIQA	HellaSwag	WinoGrande	ARC-e	ARC-c	OBQA	Avg Acc
100% LLaMA2-13B	10.98	54.42	68.99	79.05	76.60	69.77	73.32	45.56	42.00	65.04		
50% Wanda-sp	205.58	393.96	61.16	53.05	26.65	49.49	29.00	26.19	29.60	39.31		
GPrune-LLM (Wanda-sp)	<u>26.65<math>\uparrow</math></u>	<b>131.11<math>\uparrow</math></b>	61.99 $\uparrow$	<b>67.95<math>\uparrow</math></b>	<b>54.17<math>\uparrow</math></b>	54.62 $\uparrow$	<b>53.03<math>\uparrow</math></b>	<b>33.45<math>\uparrow</math></b>	<b>39.60<math>\uparrow</math></b>	<b>52.12<math>\uparrow</math></b>		
FLAP	27.91	156.91	<b>62.66</b>	65.02	48.95	<b>57.85</b>	47.43	31.48	37.00	50.06		
GPrune-LLM (FLAP)	<b>24.60<math>\uparrow</math></b>	<u>133.84<math>\uparrow</math></u>	<u>62.26</u>	<u>67.08<math>\uparrow</math></u>	<u>52.83<math>\uparrow</math></u>	<u>54.70</u>	<u>50.04<math>\uparrow</math></u>	<u>31.91<math>\uparrow</math></u>	<u>37.60<math>\uparrow</math></u>	<u>50.92<math>\uparrow</math></u>		
40% Wanda-sp	249.44	565.56	<u>61.68</u>	53.48	26.48	49.64	27.74	24.91	30.60	39.22		
GPrune-LLM (Wanda-sp)	54.18 $\uparrow$	284.64 $\uparrow$	61.65	<u>61.43<math>\uparrow</math></u>	<b>42.01<math>\uparrow</math></b>	52.01 $\uparrow$	<u>38.22<math>\uparrow</math></u>	<u>28.24<math>\uparrow</math></u>	<b>35.60<math>\uparrow</math></b>	<u>45.59<math>\uparrow</math></u>		
FLAP	<u>45.29</u>	<u>263.68</u>	<b>62.08</b>	52.98	36.90	<u>52.25</u>	38.05	27.39	34.80	43.49		
GPrune-LLM (FLAP)	<b>40.61<math>\uparrow</math></b>	<b>186.87<math>\uparrow</math></b>	58.65	<b>62.51<math>\uparrow</math></b>	<u>41.58<math>\uparrow</math></u>	<b>52.57<math>\uparrow</math></b>	<b>43.27<math>\uparrow</math></b>	<b>29.44<math>\uparrow</math></b>	<u>35.20<math>\uparrow</math></u>	<b>46.17<math>\uparrow</math></b>		
30% Wanda-sp	1943.76	3163.66	51.16	52.67	26.09	47.51	26.60	27.39	29.20	37.23		
GPrune-LLM (Wanda-sp)	<u>473.54<math>\uparrow</math></u>	<u>1137.74<math>\uparrow</math></u>	<u>51.28<math>\uparrow</math></u>	<u>56.04<math>\uparrow</math></u>	<b>30.77<math>\uparrow</math></b>	<b>51.78<math>\uparrow</math></b>	<u>32.03<math>\uparrow</math></u>	<u>28.32<math>\uparrow</math></u>	<u>32.20<math>\uparrow</math></u>	<u>40.35<math>\uparrow</math></u>		
FLAP	2676.82	3872.98	37.74	53.23	25.95	48.78	27.48	<b>28.92</b>	29.60	35.96		
GPrune-LLM (FLAP)	<b>113.96<math>\uparrow</math></b>	<b>356.34<math>\uparrow</math></b>	<b>56.64<math>\uparrow</math></b>	<b>56.58<math>\uparrow</math></b>	<u>30.45<math>\uparrow</math></u>	<u>50.28<math>\uparrow</math></u>	<b>37.92<math>\uparrow</math></b>	25.85	<b>33.20<math>\uparrow</math></b>	<b>41.56<math>\uparrow</math></b>		

Table 4: Comparison on LLaVA1.5-7B. For all metrics, higher is better.

Ratio Method	IE-percept	IE-reasoning	MMBench	MMMUScienceQA	Rel (%)
100% LLaVA1.5-7B	1454.98	300.00	61.17	35.11	64.57
90% Wanda-sp	<u>1403.68</u>	<b>283.93</b>	58.08	29.89	<u>62.66</u>
GPrune-LLM (Wanda-sp)	<b>1416.68<math>\uparrow</math></b>	<u>282.50</u>	<b>60.91<math>\uparrow</math></b>	<b>35.67<math>\uparrow</math></b>	62.28
FLAP	1232.40	254.29	54.64	32.78	60.85
GPrune-LLM (FLAP)	1380.13 $\uparrow$	270.71 $\uparrow$	<u>58.93<math>\uparrow</math></u>	<u>33.78<math>\uparrow</math></u>	<b>63.33<math>\uparrow</math></b>
80% Wanda-sp	1156.50	248.93	43.21	28.56	54.51
GPrune-LLM (Wanda-sp)	<b>1302.89<math>\uparrow</math></b>	<b>310.36<math>\uparrow</math></b>	<b>51.80<math>\uparrow</math></b>	<u>29.56<math>\uparrow</math></u>	<b>58.32<math>\uparrow</math></b>
FLAP	1032.08	237.14	47.34	28.89	<u>57.32</u>
GPrune-LLM (FLAP)	<u>1292.89<math>\uparrow</math></u>	<u>252.14<math>\uparrow</math></u>	<u>51.29<math>\uparrow</math></u>	<b>30.44<math>\uparrow</math></b>	<b>58.32<math>\uparrow</math></b>

## 4.2 Main Results

**Consistent improvement over base metrics.** GPrune-LLM consistently improves both language modeling perplexity and average accuracy on classification tasks over its respective base metric across all models and retention ratios. As shown in Tables 1–4, the  $\uparrow$  marker appears in most task columns under every

setting, indicating that the gains are broadly distributed rather than concentrated on only a few tasks. These results demonstrate that our method effectively preserves generalization ability of pruned models. Improvements are consistent across different model families and scale to the 13B model and the multimodal LLaVA setting.

**Larger gains at higher sparsity.** Performance improvements are most pronounced at aggressive pruning ratios, where calibration bias has the greatest impact. On LLaMA2-7B at 50% retention ratio, GPrune-LLM (Wanda-sp) reduces WikiText2 perplexity by over 80% from 262.32 to 50.65 and lifts average accuracy by 6.64%. Similar gains hold on Vicuna1.5-7B. The effect is most striking on LLaMA2-13B at 30% retention ratio, where the base FLAP collapses to a WikiText2 perplexity of 2676.82, while GPrune-LLM (FLAP) recovers it to 113.96 and raises average accuracy by 5.60%, demonstrating that our method prevents severe pruning failures under extreme sparsity.

**Reduced dependence on metric choice.** Across models and retention ratios, the average accuracy gap between the two base metrics shrinks substantially after applying GPrune-LLM. On Vicuna1.5-7B, the gap closes from 2.80% to just 0.30% at 70%, a reduction of nearly 90%, with consistent compression observed across all other models and ratios. This convergence indicates that one major source of performance disparity between importance metrics is calibration-induced ranking distortion, which our framework corrects at the structural level.

**Comparable inference speedup.**

Table 5 reports practical inference throughput at 50% retention ratio on LLaMA2-7B. Inference throughput is measured with prompt length 2048, generation length 512, and batch size 8, averaged over 10 runs. All pruned models achieve over 50% throughput improvement over the dense baseline, and GPrune-LLM achieves comparable practical speedup to its respective base metrics.

Table 5: Practical inference speedup.

Retention Ratio	Method	Params	Tokens/s
100%	LLaMA2-7B	6.74B	97.04
50%	LLM-Pruner	3.45B	161.69
	Wanda-sp	3.5B	167.44
	GPrune-LLM (Wanda-sp)	3.5B	165.45
	FLAP	3.5B	148.52
	GPrune-LLM (FLAP)	3.5B	150.44

### 4.3 Ablation Study

**Calibration Datasets** We evaluate GPrune-LLM under all pairwise combinations of three commonly-used calibration datasets: WikiText2 [28] (Wikipedia articles), PTB [27] (Wall Street Journal financial text), and C4 [31] (large-scale web-crawled text). These three datasets span clearly distinct domains, with C4 and PTB representing the largest distributional contrast and WikiText2 falling between the two. Results are shown in Table 6.

GPrune-LLM consistently outperforms the corresponding FLAP baseline that uses a single calibration dataset across all six pairings in average accuracy. This confirms that cross-dataset rank drift is a reliable behavior signal across different dataset choices.

Table 6: Comparison under different calibration datasets at 50% retention ratio on LLaMA2-7B. For calibration pairs  $A+B$ ,  $A$  is the primary dataset used for importance scoring and sparsity learning, while  $B$  is the auxiliary one only used to compute rank drift for neuron behavior inference and does not guide pruning decisions directly.

Method	Calibration	WikiText2 PPL	PTB PPL	BoolQ	PIQA	HellaSwag	WinoGrande	ARC-e	ARC-c	OBQA	Avg Acc
FLAP	WikiText2	42.81	152.49	39.63	62.13	39.54	50.36	35.52	28.24	35.20	41.52
GPrune-LLM (FLAP)	WikiText2+ PTB	<u>33.92</u> ↑	<u>129.06</u> ↑	51.13↑	63.60↑	45.01↑	<u>52.49</u> ↑	<u>43.52</u> ↑	<b>29.35</b> ↑	34.80	45.70↑
GPrune-LLM (FLAP)	WikiText2+ C4	<b>33.33</b> ↑	127.55↑	45.50↑	64.15↑	45.24↑	50.75↑	40.95↑	28.16	34.60	44.19↑
FLAP	PTB	63.87	<b>119.61</b>	38.23	59.85	36.67	51.54	37.79	26.96	32.80	40.55
GPrune-LLM (FLAP)	PTB+ WikiText2	61.29↑	120.94	57.86↑	61.53↑	39.60↑	50.75	38.34↑	26.71	33.60↑	44.06↑
GPrune-LLM (FLAP)	PTB+ C4	62.77↑	123.04	<b>60.89</b> ↑	62.73↑	40.02↑	50.83	40.07↑	27.39↑	33.60↑	45.08↑
FLAP	C4	91.78	217.40	39.05	66.10	46.54	50.36	38.80	<u>29.10</u>	<u>35.60</u>	43.65
GPrune-LLM (FLAP)	C4+ WikiText2	73.88↑	211.14↑	54.40↑	<u>69.53</u> ↑	<u>49.86</u> ↑	<b>53.75</b> ↑	41.71↑	28.16	<b>36.00</b> ↑	<u>47.63</u> ↑
GPrune-LLM (FLAP)	C4+ PTB	76.01↑	214.31↑	<u>60.28</u> ↑	<b>69.64</b> ↑	<b>50.09</b> ↑	52.17↑	<b>44.70</b> ↑	28.75	35.20	<b>48.69</b> ↑

The diversity of the primary calibration dataset affects absolute performance. When C4 serves as primary, GPrune-LLM achieves the two highest results in the table, reaching 47.63% average accuracy with C4+WikiText2 and 48.69% with C4+PTB, reflecting C4’s broader distributional coverage as a basis for importance scoring. WikiText2 and PTB as primary yield lower absolute performance, consistent with their narrower domain coverage.

The domain contrast between primary and auxiliary further amplifies improvements. When C4 is primary, the PTB auxiliary produces the largest single improvement in the table at 5.04%, and when PTB is primary, pairing with C4 outperforms pairing with WikiText2 by 1.02%. Greater distributional contrast yields more discriminative rank drift signals, enabling more accurate behavior-based module separation.

**Components** We ablate the two stages of GPrune-LLM on Wanda-sp at 50% retention ratio on LLaMA2-7B. Wanda-sp is used as it yields the largest total gain of 6.64% in average accuracy, making individual contributions more visible. Results are shown in Table 7.

**Behavior-consistent modularization.** With module initialization only, plus full reliability-aware modular pruning, average accuracy recovers substantially to 45.04%. Differentiable refinement further improves average accuracy to 46.01% and reduces perplexity on both datasets, as joint optimization over parameter similarity and rank drift consistency yields more behavior-consistent module assignments.

**Reliability-aware modular pruning.** Removing metric adaptation drops average accuracy by 1.93% to 44.08% and slightly worsens both perplexity metrics, as certain distribution-sensitive modules are left with activation-based metrics

Table 7: Component ablation of GPrune-LLM on Wanda-sp at 50% retention ratio on LLaMA2-7B.

Behavior-consistent Modularization		Reliability-aware Modular Pruning		WikiText2 PPL	PTB PPL	Avg Acc
Module Initialization	Differentiable Refinement	Metric Adaptation	Adaptive Sparsity Learning			
				262.32	505.51	39.37
✓		✓	✓	55.29	180.07	45.04
✓	✓		✓	53.99	181.57	44.08
✓	✓	✓		174.63	577.00	41.65
✓	✓	✓	✓	<b>50.65</b>	<b>172.26</b>	<b>46.01</b>

that produce unreliable rankings. Adaptive sparsity learning is responsible for translating the modular structure into a valid pruned model under a global sparsity budget. Without learnable per-module thresholds, the retention ratios are suboptimal, and its removal causes dramatic degradation across all metrics, with WikiText2 perplexity rising from 50.65 to 174.63, PTB perplexity from 172.26 to 577.00, and average accuracy collapsing by 4.36% to 41.65%.

All components contribute, and the two stages are mutually reinforcing, as behavior-consistent modularization provides the structural foundation that makes per-module reliability assessment and adaptive sparsity learning effective.

**Epoch Number** We study the effect of threshold training epochs in adaptive sparsity learning across sparsity levels. Results are shown in Fig. 3.

At 80% and 70% retention ratios, WikiText2 perplexity remains stable after epoch 1, indicating rapid convergence at mild sparsity. At 50% retention ratio, perplexity starts substantially higher and continues to improve over all three epochs. This reflects the increased difficulty of threshold learning under aggressive sparsity, and confirms that higher sparsity requires more training epochs.

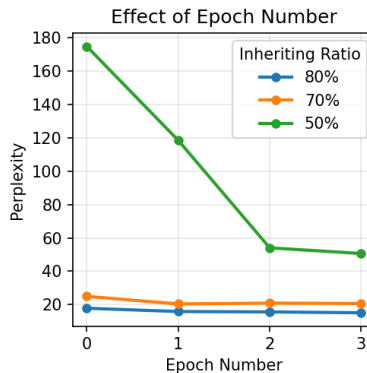


Fig. 3: Effect of threshold training epoch number in adaptive sparsity learning on WikiText2 perplexity at different retention ratios on LLaMA2-7B with Wanda-sp.

## 5 Conclusion

We presented GPrune-LLM, which identifies two structural limitations of existing activation-based structured pruning methods, namely cross-behavior ranking

interference and local ranking distortion, and addresses them through behavior-consistent modularization and reliability-aware modular pruning. Experiments across LLaMA families, Vicuna, and LLaVA show consistent improvement over base importance metrics at all retention ratios, with larger gains at high sparsity and substantially reduced dependence on metric choice, demonstrating that properly restructuring the neuron ranking space is essential to preserving the generalization ability of LLMs in structured pruning.

## References

1. An, Y., Zhao, X., Yu, T., Tang, M., Wang, J.: Fluctuation-based adaptive structured pruning for large language models. In: Proceedings of the AAAI Conference on Artificial Intelligence. vol. 38, pp. 10865–10873 (2024)
2. Ashkboos, S., Croci, M.L., Gennari do Nascimento, M., Hoefler, T., Hensman, J.: Slicept: Compress large language models by deleting rows and columns. In: The Twelfth International Conference on Learning Representations. OpenReview (2024)
3. Ban, Z., Ma, H., Zhang, S., Liu, S., Chen, X., Yang, M.: Gap: a global adaptive pruning method for large language models. In: Proceedings of the 2025 Conference on Empirical Methods in Natural Language Processing. pp. 20909–20914 (2025)
4. Bandari, A., Yin, L., Hsieh, C.Y., Jaiswal, A.K., Chen, T., Shen, L., Krishna, R., Liu, S.: Is c4 dataset optimal for pruning? an investigation of calibration data for llm pruning. In: Proceedings of the 2024 Conference on Empirical Methods in Natural Language Processing. pp. 18089–18099 (2024)
5. Bisk, Y., Zellers, R., Gao, J., Choi, Y., et al.: Piqa: Reasoning about physical commonsense in natural language. In: Proceedings of the AAAI conference on artificial intelligence. vol. 34, pp. 7432–7439 (2020)
6. Chen, Y., Cheng, B., Han, J., Zhang, Y., Li, Y., Zhang, S.: Dlp: Dynamic layer-wise pruning in large language models. In: International Conference on Machine Learning. pp. 7934–7956. PMLR (2025)
7. Clark, C., Lee, K., Chang, M.W., Kwiatkowski, T., Collins, M., Toutanova, K.: Boolq: Exploring the surprising difficulty of natural yes/no questions. In: Proceedings of the 2019 conference of the north American chapter of the association for computational linguistics: Human language technologies, volume 1 (long and short papers). pp. 2924–2936 (2019)
8. Clark, P., Cowhey, I., Etzioni, O., Khot, T., Sabharwal, A., Schoenick, C., Tafjord, O.: Think you have solved question answering? try arc, the ai2 reasoning challenge. arXiv preprint arXiv:1803.05457 (2018)
9. Dong, P., Li, L., Tang, Z., Liu, X., Pan, X., Wang, Q., Chu, X.: Pruner-zero: Evolving symbolic pruning metric from scratch for large language models. In: International Conference on Machine Learning. pp. 11346–11374. PMLR (2024)
10. Duan, H., Yang, J., Qiao, Y., Fang, X., Chen, L., Liu, Y., Dong, X., Zang, Y., Zhang, P., Wang, J., et al.: Vlmevalkit: An open-source toolkit for evaluating large multi-modality models (2024)
11. Frantar, E., Alistarh, D.: Sparsegpt: Massive language models can be accurately pruned in one-shot. In: International conference on machine learning. pp. 10323–10337. PMLR (2023)

12. Fu, C., Chen, P., Shen, Y., Qin, Y., Zhang, M., Lin, X., Yang, J., Zheng, X., Li, K., Sun, X., et al.: Mme: A comprehensive evaluation benchmark for multimodal large language models. arXiv preprint arXiv:2306.13394 (2023)
13. Gao, L., Tow, J., Biderman, S., Black, S., DiPofi, A., Foster, C., Golding, L., Hsu, J., McDonell, K., Muennighoff, N., et al.: A framework for few-shot language model evaluation. Zenodo (2021)
14. Geva, M., Schuster, R., Berant, J., Levy, O.: Transformer feed-forward layers are key-value memories. In: Proceedings of the 2021 Conference on Empirical Methods in Natural Language Processing. pp. 5484–5495 (2021)
15. Grattafiori, A., Dubey, A., Jauhri, A., Pandey, A., Kadian, A., Al-Dahle, A., Letman, A., Mathur, A., Schelten, A., Vaughan, A., et al.: The llama 3 herd of models (2024)
16. Hinton, G., Vinyals, O., Dean, J.: Distilling the knowledge in a neural network. arXiv preprint arXiv:1503.02531 (2015)
17. Hubara, I., Courbariaux, M., Soudry, D., El-Yaniv, R., Bengio, Y.: Binarized neural networks. Advances in neural information processing systems **29** (2016)
18. Ji, Y., Xiang, Y., Li, J., Xia, Q., Li, P., Duan, X., Wang, Z., Zhang, M.: Beware of calibration data for pruning large language models. In: The Thirteenth International Conference on Learning Representations (2025)
19. Junjie, L., Zhe, X., Runbin, S., Hayden, K.: Dynamic sparse training: Find efficient sparse network from scratch with trainable masked layers. In: 8th International Conference on Learning Representations (ICLR 2020). International Conference on Learning Representations, ICLR (2020)
20. Kim, M.J., Pertsch, K., Karamcheti, S., Xiao, T., Balakrishna, A., Nair, S., Rafailov, R., Foster, E., Lam, G., Sanketi, P., et al.: Openvla: An open-source vision-language-action model. arXiv preprint arXiv:2406.09246 (2024)
21. Liu, H., Li, C., Li, Y., Lee, Y.J.: Improved baselines with visual instruction tuning. In: Proceedings of the IEEE/CVF conference on computer vision and pattern recognition. pp. 26296–26306 (2024)
22. Liu, H., Li, C., Wu, Q., Lee, Y.J.: Visual instruction tuning. vol. 36, pp. 34892–34916 (2023)
23. Liu, Y., Duan, H., Zhang, Y., Li, B., Zhang, S., Zhao, W., Yuan, Y., Wang, J., He, C., Liu, Z., et al.: Mmbench: Is your multi-modal model an all-around player? pp. 216–233 (2024)
24. Lloyd, S.: Least squares quantization in pcm. IEEE transactions on information theory **28**(2), 129–137 (1982)
25. Lu, P., Mishra, S., Xia, T., Qiu, L., Chang, K.W., Zhu, S.C., Tafjord, O., Clark, P., Kalyan, A.: Learn to explain: Multimodal reasoning via thought chains for science question answering. vol. 35, pp. 2507–2521 (2022)
26. Ma, X., Fang, G., Wang, X.: Llm-pruner: On the structural pruning of large language models. Advances in neural information processing systems **36**, 21702–21720 (2023)
27. Marcus, M., Santorini, B., Marcinkiewicz, M.A.: Building a large annotated corpus of english: The penn treebank. Computational linguistics **19**(2), 313–330 (1993)
28. Merity, S., Xiong, C., Bradbury, J., Socher, R.: Pointer sentinel mixture models. In: International Conference on Learning Representations (2017)
29. Mihaylov, T., Clark, P., Khot, T., Sabharwal, A.: Can a suit of armor conduct electricity? a new dataset for open book question answering. In: Proceedings of the 2018 conference on empirical methods in natural language processing. pp. 2381–2391 (2018)

30. Qiu, Z., Huang, Z., Fu, J.: Unlocking emergent modularity in large language models. In: Proceedings of the 2024 Conference of the North American Chapter of the Association for Computational Linguistics: Human Language Technologies (Volume 1: Long Papers). pp. 2638–2660 (2024)
31. Raffel, C., Shazeer, N., Roberts, A., Lee, K., Narang, S., Matena, M., Zhou, Y., Li, W., Liu, P.J.: Exploring the limits of transfer learning with a unified text-to-text transformer. *Journal of machine learning research* **21**(140), 1–67 (2020)
32. Sakaguchi, K., Bras, R.L., Bhagavatula, C., Choi, Y.: Winogrande: An adversarial winograd schema challenge at scale. vol. 64, pp. 99–106. ACM New York, NY, USA (2021)
33. Sun, M., Liu, Z., Bair, A., Kolter, J.Z.: A simple and effective pruning approach for large language models. In: 12th International Conference on Learning Representations, ICLR 2024 (2024)
34. Touvron, H., Martin, L., Stone, K., Albert, P., Almahairi, A., Babaei, Y., Bashlykov, N., Batra, S., Bhargava, P., Bhosale, S., et al.: Llama 2: Open foundation and fine-tuned chat models. arXiv preprint arXiv:2307.09288 (2023)
35. Wang, P., Bai, S., Tan, S., Wang, S., Fan, Z., Bai, J., Chen, K., Liu, X., Wang, J., Ge, W., et al.: Qwen2-vl: Enhancing vision-language model’s perception of the world at any resolution. arXiv preprint arXiv:2409.12191 (2024)
36. Wei, J., Lu, Q., Jiang, N., Li, S., Xiang, J., Chen, J., Liu, Y.: Structured optimal brain pruning for large language models. In: Proceedings of the 2024 Conference on Empirical Methods in Natural Language Processing. pp. 13991–14007 (2024)
37. Williams, M., Aletras, N.: On the impact of calibration data in post-training quantization and pruning. In: Proceedings of the 62nd Annual Meeting of the Association for Computational Linguistics (Volume 1: Long Papers). pp. 10100–10118 (2024)
38. Wu, G., Zhang, H., Zhibin, Z., Guo, J., Cheng, X.: Iterative structured pruning for large language models with multi-domain calibration. arXiv preprint arXiv:2601.02674 (2026)
39. Yin, L., Wu, Y., Zhang, Z., Hsieh, C.Y., Wang, Y., Jia, Y., Li, G., Jaiswal, A., Pechenizkiy, M., Liang, Y., et al.: Outlier weighed layerwise sparsity (owl) a missing secret sauce for pruning llms to high sparsity. In: Proceedings of the 41st International Conference on Machine Learning. pp. 57101–57115 (2024)
40. Yu, T., An, Y., Zhu, K., Zhu, G., Tang, M., Wang, J.: Improving generalization in llm structured pruning via function-aware neuron grouping. arXiv preprint arXiv:2512.23014 (2025)
41. Yue, X., Ni, Y., Zhang, K., Zheng, T., Liu, R., Zhang, G., Stevens, S., Jiang, D., Ren, W., Sun, Y., et al.: Mmmu: A massive multi-discipline multimodal understanding and reasoning benchmark for expert agi. In: Proceedings of the IEEE/CVF conference on computer vision and pattern recognition. pp. 9556–9567 (2024)
42. Zellers, R., Holtzman, A., Bisk, Y., Farhadi, A., Choi, Y.: Hellaswag: Can a machine really finish your sentence? In: Proceedings of the 57th annual meeting of the association for computational linguistics. pp. 4791–4800 (2019)
43. Zhang, H., XiaolongShi, X., Sun, J., Sun, G.: Structured pruning for large language models using coupled components elimination and minor fine-tuning. In: Findings of the Association for Computational Linguistics: NAACL 2024. pp. 1–12 (2024)
44. Zhang, M., Chen, H., Shen, C., Yang, Z., Ou, L., Yu, X., Zhuang, B.: Loraprune: Structured pruning meets low-rank parameter-efficient fine-tuning. In: Findings of the Association for Computational Linguistics: ACL 2024. pp. 3013–3026 (2024)

45. Zhang, Z., Lin, Y., Liu, Z., Li, P., Sun, M., Zhou, J.: Moefication: Transformer feed-forward layers are mixtures of experts. In: Findings of the Association for Computational Linguistics: ACL 2022. pp. 877–890 (2022)
46. Zhang, Z., Zeng, Z., Lin, Y., Xiao, C., Wang, X., Han, X., Liu, Z., Xie, R., Sun, M., Zhou, J.: Emergent modularity in pre-trained transformers. In: Findings of the Association for Computational Linguistics: ACL 2023. pp. 4066–4083 (2023)

Table 8: Hyperparameters of GPrune-LLM. BCM denotes Behavior-consistent Modularization, including Module Initialization (MI) and Differentiable Refinement (DR). RMP denotes Reliability-aware Modular Pruning, including Metric Adaptation (MA) and Adaptive Sparsity Learning (ASL).

Stage	Substage	Parameter	Value
General		Calibration sample number $ \mathcal{D} $	2048
		Sequence length	128
		Primary calibration dataset	WikiText2
		Auxiliary calibration dataset	PTB
BCM	MI	Candidate module numbers $\mathcal{K}$	{16, 24, 32, 40, 48}
		Drift-std split quantile $\gamma_{\text{split}}$	0.80
		Minimum module size for split	32
BCM	DR	Refinement steps	15
		Refinement learning rate (Adam)	0.01
		Worst-module quantile $\gamma_{\text{pair}}$	0.25
RMP	MA	Drift threshold quantile $\gamma_{\text{drift}}$	0.90
		Score threshold quantile $\gamma_{\text{score}}$	0.90
	ASL	Threshold learning rate (Adam)	0.01
		Quadratic penalty $\rho_{\text{pen}}$	0.05
		Dual variable update rate $\rho_{\text{lam}}$	0.02

Table 9: Training epochs for adaptive sparsity learning per model, metric, and retention ratio, listed from high to low following the main paper tables.

Model	Metric	Training Epochs		
		R1	R2	R3
LLaMA1-7B (80%/70%/50%)	Wanda-sp	0.5	1	3
	FLAP	1	0.5	1
LLaMA2-7B (80%/70%/50%)	Wanda-sp	1	1	3
	FLAP	3	3	3
Vicuna1.5-7B (80%/70%/50%)	Wanda-sp	0.5	1	3
	FLAP	2	2	1
LLaMA2-13B (50%/40%/30%)	Wanda-sp	3	3	4
	FLAP	2	3	2
LLaVA1.5-7B (90%/80%)	Wanda-sp	3	3	—
	FLAP	3	3	—

Table 10: Comparison on LLaMA2-7B at 40% retention ratio. The best and second-best results are marked in **bold** and underline, respectively.  $\uparrow$  denotes improvement over the corresponding base method at the same retention ratio. For language modeling perplexity, lower is better. For classification task accuracy, higher is better.

Ratio	Method	WikiText2 PPL	PTB PPL	BoolQ	PIQA	HellaSwag	WinoGrande	ARC-e	ARC-c	OBQA	Avg Acc
100%	LLaMA2-7B	12.19	48.35	71.10	78.40	72.96	67.25	69.36	40.53	40.80	62.91
40%	LLM-Pruner	547.02	1112.72	<u>59.51</u>	55.88	26.67	47.91	27.99	25.00	29.00	38.85
	Wanda-sp	938.11	1150.68	47.55	52.77	25.98	49.09	26.85	25.85	31.60	37.10
	GPrune-LLM (Wanda-sp)	197.41 $\uparrow$	567.45 $\uparrow$	<b>61.25<math>\uparrow</math></b>	<u>56.53<math>\uparrow</math></u>	<u>31.47<math>\uparrow</math></u>	<b>51.30<math>\uparrow</math></b>	31.82 $\uparrow$	<b>29.27<math>\uparrow</math></b>	31.40 $\uparrow$	<b>41.86<math>\uparrow</math></b>
	FLAP	<u>118.07</u>	<u>301.23</u>	43.09	<u>58.22</u>	30.23	48.22	<u>33.54</u>	26.45	<u>33.00</u>	38.96
	GPrune-LLM (FLAP)	<b>64.21<math>\uparrow</math></b>	<b>226.78<math>\uparrow</math></b>	45.41 $\uparrow$	<b>59.52<math>\uparrow</math></b>	<b>36.42<math>\uparrow</math></b>	<u>49.72<math>\uparrow</math></u>	<b>36.95<math>\uparrow</math></b>	<u>27.39<math>\uparrow</math></u>	<b>33.40<math>\uparrow</math></b>	<u>41.26<math>\uparrow</math></u>

## A Appendix

## B Detailed Experimental Settings

Table 8 provides detailed hyperparameter settings used in experiments reported in the main paper.

Table 9 lists the training epoch number settings for adaptive sparsity learning, which vary across models, pruning metrics, and retention ratios. Epoch numbers are determined empirically by monitoring perplexity on the calibration set. The general trend is that higher sparsity requires more epochs, which is more obvious for Wanda-sp, reflecting the increased difficulty of threshold learning under aggressive sparsity.

## C LLaMA2-7B Results at Extreme Sparsity

The main paper evaluates LLaMA2-7B at 80%, 70%, and 50% retention ratios. Table 10 extends this to a more extreme 40% setting where calibration bias is most severe. At this ratio, Wanda-sp’s WikiText2 perplexity collapses to 938.11, while GPrune-LLM (Wanda-sp) recovers it to 197.41, a reduction of nearly 80%. FLAP is more resilient, achieving a WikiText2 perplexity of 118.07, which GPrune-LLM (FLAP) further reduces to 64.21. The two GPrune-LLM variants rank first and second in average accuracy at 41.86% and 41.26%, respectively, and the gap between the two base metrics narrows from 1.86% to 0.60%, consistent with the main paper findings.

## D LLaMA1-7B Results

Table 11 reports results on LLaMA1-7B. GPrune-LLM consistently improves over the corresponding base metric across all retention ratios, consistent with the main paper. However, the gains are more modest than those observed on LLaMA2 and later models.

Table 11: Comparison on LLaMA1-7B.

Ratio Method	WikiText2 PPL	PTB PPL	BoolQ	PIQA	HellaSwag	WinoGrande	ARC-e	ARC-c	OBQA	Avg Acc
100% LLaMA1-7B	12.62	53.83	73.18	78.35	73.00	66.93	67.30	41.47	42.40	63.23
80% LLM-Pruner	19.99	79.68	64.19	<b>75.68</b>	66.56	59.19	61.91	36.60	<b>40.80</b>	57.85
Wanda-sp	16.54	79.35	<b>71.59</b>	<u>75.63</u>	<u>67.86</u>	<u>65.67</u>	61.78	<u>38.05</u>	38.60	<u>59.88</u>
GPrune-LLM (Wanda-sp)	15.68↑	74.43↑	<u>70.98</u>	75.30	<b>68.28</b> ↑	<b>66.93</b> ↑	<u>64.35</u> ↑	<b>38.57</b> ↑	38.00	<b>60.34</b> ↑
FLAP	<u>15.04</u>	<b>66.92</b>	68.72	74.86	64.97	64.88	63.09	37.30	<u>39.40</u>	59.03
GPrune-LLM (FLAP)	<b>14.94</b> ↑	<u>68.47</u>	70.21↑	<u>75.63</u> ↑	66.17↑	64.00	<b>64.52</b> ↑	37.29	<b>40.80</b> ↑	59.80↑
70% LLM-Pruner	30.14	114.40	53.49	<b>72.20</b>	59.05	57.06	54.59	<b>34.98</b>	38.40	52.82
Wanda-sp	21.39	107.91	63.98	71.33	<u>59.48</u>	<b>60.69</b>	57.15	34.30	38.20	55.02
GPrune-LLM (Wanda-sp)	18.52↑	83.52↑	61.07	71.55↑	<b>60.74</b> ↑	<u>60.06</u>	<u>59.72</u> ↑	34.39↑	<u>39.60</u> ↑	<u>55.30</u> ↑
FLAP	<u>18.33</u>	<u>79.38</u>	<u>64.80</u>	70.78	58.30	59.04	57.15	34.56	37.60	54.60
GPrune-LLM (FLAP)	<b>17.31</b> ↑	<b>78.50</b> ↑	<b>65.90</b> ↑	<u>72.14</u> ↑	59.39↑	59.83↑	<b>61.95</b> ↑	<u>34.81</u> ↑	<b>39.80</b> ↑	<b>56.26</b> ↑
50% LLM-Pruner	118.10	402.75	56.48	60.99	35.78	52.01	34.13	27.73	34.20	43.05
Wanda-sp	269.13	633.01	40.70	54.46	28.31	49.72	28.62	23.46	30.60	36.55
GPrune-LLM (Wanda-sp)	79.01↑	324.52↑	61.65↑	55.77↑	29.76↑	50.20↑	32.70↑	22.10	31.80↑	40.57↑
FLAP	<u>32.73</u>	<u>165.31</u>	<u>61.80</u>	<u>63.00</u>	<u>41.78</u>	<b>55.01</b>	<u>45.79</u>	<u>30.03</u>	<u>35.40</u>	<u>47.54</u>
GPrune-LLM (FLAP)	<b>30.81</b> ↑	<b>134.21</b> ↑	<b>62.17</b> ↑	<b>64.42</b> ↑	<b>43.10</b> ↑	<u>52.88</u>	<b>47.18</b> ↑	<b>31.83</b> ↑	<b>35.80</b> ↑	<b>48.20</b> ↑

Table 12: Module separation score on the WikiText2-PTB pair. Larger values indicate clearer module-level separation in cross-dataset rank drift.

Model	FLAP	Wanda-sp
LLaMA1-7B	0.9249	0.9135
LLaMA2-7B	0.9714	0.9723

One possible explanation is that LLaMA1 exhibits weaker neuron modularity than LLaMA2 and later models, potentially due to differences in pretraining scale and data diversity. In that case, cross-dataset rank-drift patterns would be less structured, making BCM less likely to produce clearly separated modules and thus reducing the gains.

To quantify this, we define a module separation score (MSS). For neuron  $i$ , let  $d_i$  denote its rank drift between WikiText2 and PTB. For module  $m$ , let  $\mu_m = \frac{1}{|m|} \sum_{i \in m} d_i$  be the module-level mean drift and  $\sigma_m = \text{Std}_{i \in m}(d_i)$  be the within-module drift dispersion. MSS is defined as the ratio of between-module to within-module drift variation:

$$\text{MSS} = \frac{\text{Std}_m(\mu_m)}{\frac{1}{M} \sum_{m=1}^M \sigma_m}, \quad (12)$$

where  $M$  is the number of modules. A higher MSS indicates that modules are more distinctly separated in terms of cross-dataset rank-drift behavior.

Table 12 shows that LLaMA1-7B exhibits lower MSS than LLaMA2-7B under both metrics, indicating less distinct module-level separation. This offers a plausible explanation for the reduced improvement margins in Table 11.

Table 13: Cross-dataset module overlap on LLaMA2-7B.

Dataset-pair comparison	Global matched acc.	Global matched IoU
WikiText2-PTB vs. WikiText2-C4	0.6923	0.4733
WikiText2-C4 vs. PTB-C4	0.7009	0.4866
PTB-C4 vs. WikiText2-PTB	0.6936	0.4725

## E Cross-Dataset Module Overlap

BCM derives the modular structure from rank drift between a pair of calibration datasets. A natural question is whether the resulting modules reflect a general property of the model. To investigate, we compare module assignments produced by three different dataset pairs. Since module labels are arbitrary across modularizations, we first align them via optimal one-to-one matching.

Let  $A_m$  and  $B_m$  denote the neuron sets of the aligned module pair  $m$ , and  $N$  the total neuron count. Matched accuracy

$$\text{Acc}_{\text{match}} = \frac{\sum_m |A_m \cap B_m|}{N} \quad (13)$$

measures the fraction of neurons with consistent assignments across modularizations. Matched IoU

$$\text{IoU}_{\text{match}} = \frac{1}{M} \sum_{m=1}^M \frac{|A_m \cap B_m|}{|A_m \cup B_m|} \quad (14)$$

measures boundary cleanliness and is more sensitive to cross-module mixing.

Table 13 reports results across all three dataset-pair comparisons. The global matched accuracy is consistently around 0.70, and the global matched IoU is around 0.48.

First, the matched accuracy above 0.69 indicates that roughly 70% of neurons receive consistent module assignments regardless of which dataset pair is used. This level of overlap is well above chance and suggests that the modular structure learned by BCM is not merely an artifact of the specific calibration pair, but reflects a more general property of the model’s neuron organization. The two-dataset BCM used in this work is therefore reasonably representative.

Second, approximately 30% of neurons shift module assignment across dataset pairs, and matched IoU remains around 0.48, indicating that module boundaries are not fully invariant to dataset choice. Exploiting more distributionally diverse calibration data during the BCM stage may yield more stable boundaries and further improve the framework.